CHEMISTRY
A EUROPEAN JOURNAL

Rotational Dynamics Account for pH-Dependent Relaxivities of PAMAM Dendrimeric, Gd-Based Potential MRI Contrast Agents

Sabrina Laus, Angélique Sour, Robert Ruloff, Éva Tóth, and André E. Merbach*[a]

Abstract: The $EPTPA^{5-}$ chelate, which ensures fast water exchange in Gd^{III} complexes, has been coupled to three different generations (5, 7, and 9) of polyamidoamine (PAMAM) dendrimers through benzylthiourea linkages (H_5EPTPA = ethylenepropylenetriamine-*N*,*N*,*N*′,*N*″,*N*″-pentaacetic acid). The proton relaxivities measured at pH 7.4 for the dendrimer complexes G5-$(GdEPTPA)_{111}$, G7-$(GdEPTPA)_{253}$ and G9-$(GdEPTPA)_{1157}$ decrease with increasing temperature, indicating that, for the first time for dendrimers, slow water exchange does not limit relaxivity. At a given field and temperature, the relaxivity increases from G5 to G7, and then slightly decreases for G9 (r_1 = 20.5, 28.3 and 27.9 $mM^{-1}s^{-1}$, respectively, at 37 °C, 30 MHz). The relaxivities show a strong and reversible pH dependency for all three dendrimer complexes. This originates from the pH-dependent rotational dynamics of the dendrimer skeleton, which was evidenced by a combined variable-temperature and multiple-field ^{17}O NMR and ^{1}H relaxivity study performed at pH 6.0 and 9.9 on G5-$(GdEPTPA)_{111}$. The longitudinal ^{17}O and ^{1}H relaxation rates of the dendrimeric complex are strongly pH-dependent, whereas they are not for the $[Gd(EPTPA)(H_2O)]^{2-}$ monomer chelate. The longitudinal ^{17}O and ^{1}H relaxation rates have been analysed by the Lipari–Szabo spectral density functions and correlation times have been calculated for the global motion of the entire macromolecule (τ_{gO}) and the local motion of the Gd^{III} chelates on the surface (τ_{lO}), correlated by means of an order parameter S^2. The dendrimer complex G5-$(GdEPTPA)_{111}$ has a considerably higher τ_{gO} under acidic than under basic conditions (τ_{gO}^{298} = 4040 ps and 2950 ps, respectively), while local motions are less influenced by pH (τ_{lO}^{298} = 150 and 125 ps). The order parameter, characterizing the rigidity of the macromolecule, is also higher at pH 6.0 than at pH 9.9 (S^2 = 0.43 vs 0.36, respectively). The pH dependence of the global correlation time can be related to the protonation of the tertiary amine groups in the PAMAM skeleton, which leads to an expanded and more rigid dendrimeric structure at lower pH. The increase of τ_{gO} with decreasing pH is responsible for the pH dependent proton relaxivities. The water exchange rate on G5-$(GdEPTPA)_{111}$ ($k_{ex}^{298} = 150 \times 10^6\ s^{-1}$) shows no significant pH dependency and is similar to the one measured for the monomer $[Gd(EPTPA)(H_2O)]^{2-}$. The proton relaxivity of G5-$(GdEPTPA)_{111}$ is mainly limited by the important flexibility of the dendrimer structure, and to a small extent, by a faster than optimal water exchange rate.

Keywords: dendrimers · gadolinium · imaging agents · rotational dynamics · water exchange

Introduction

Dendrimers represent an important class of synthetic polymeric nanostructures, and have become an important field of research for biomedical applications.[1] The potential of dendrimers in this area covers a large spectrum and involves drug delivery (transfection agents for DNA delivery into cells, glycocarriers)[2–5] antiviral treatment (naphtyl-sulfonate-loaded dendrimers show anti-HIV activity),[6] antibacterial drugs (dendrimers derivatised with tertiary alkyl ammonium groups are potent antibacterial biocides against Gram-positive and negative bacteria)[7,8] or antitumor activity (photosensitisers coupled to dendrimers).[9] The diversity of possible biomedical applications results from the fact that the core, the interior and the surface functionalities of a dendrimer can be all tuned to a desired objective.

Polyamidoamine (PAMAM) dendrimers are highly branched, water-soluble, spheroidal nanoparticles. They are

[a] S. Laus, Dr. A. Sour, Dr. R. Ruloff, Dr. É. Tóth, Prof. A. E. Merbach
Ecole Polytechnique Fédérale de Lausanne (EPFL)
Laboratoire de Chimie Inorganique et Bioinorganique
EPFL-BCH, 1015 Lausanne (Switzerland)
Fax: (+41) 21-693-9875
E-mail: andre.merbach@epfl.ch

Supporting information for this article is available on the WWW under http://www.chemeurj.org/ or from the author.

DOI: 10.1002/chem.200401326

composed of a core (generally ammonia or aliphatic diamine), repeated polyamidoamine units, and different types of functional groups (e.g., primary amines) on the surface. They are produced in successive generations with well-defined molecular weight, diameter and number of primary amino groups on the surface. The pronounced branching provides the higher generations with an increasingly three-dimensional structure that is characterised by a growing number of cavities within the molecule.[10] For intermediate generations (G4–6), these cavities are accessible, while higher generations manifest limited surface permeability.[11] The total number of reactive functional groups on a dendrimer surface depends on the number of reactive groups in the core, on the branch cell multiplicity and on the generation. In the PAMAM dendrimer family, initiated from an ethylenediamine core, the number of terminal amino groups is 128, 512 and 2048 for G5, G7 and G9, respectively.[12] Non-toxicity is of crucial importance; it has been shown on mice that PAMAM-based dendrimers do not exhibit properties that would exclude their use in biological applications.[13]

During the last two decades, medical magnetic resonance imaging (MRI) has evolved into one of the most efficient diagnostic techniques. This progress has been largely assisted by the successful use of paramagnetic contrast agents, Gd^{III} complexes in the majority. The design of highly efficient agents can only be achieved on a rational basis, considering the relationship between structure, dynamics and the relevant parameters determining relaxation processes. The Solomon–Bloembergen–Morgan theory which correlates the observed paramagnetic relaxation rate enhancement to microscopic properties predicts maximum proton relaxivities for Gd^{III} complexes when the three most important influencing factors, rotation, water exchange, and electron-spin relaxation are simultaneously optimised.[14] Proton relaxivity (r_1) is defined as the increase in longitudinal water proton relaxation rate per millimolar concentration of Gd^{III}. The relaxivity can be theoretically increased to over $100\,mM^{-1}s^{-1}$ for monohydrated chelates instead of $r_1 = 4$–$5\,mM^{-1}s^{-1}$ for the current, commercial agents.

With the aim of optimizing proton relaxivity, the tumbling time of the Gd^{III} complexes has to be increased; this can be achieved by macromolecular assemblies. In addition, conjugation to large macromolecules is an approach to alter biophysical and pharmacological properties of the metal chelate, such as blood retention, tissue perfusion or excretion.[15] For example, macromolecular agents tend to be retained in the vascular space by virtue of their size, hence they are useful for blood-pool imaging by magnetic resonance angiography[16–18] or for evaluation of the microvasculature in tumour tissues.[19,20] The conjugation of low-molecular-weight chelates to macromolecules can be achieved through different ways, involving linear polymers,[21–25] dendrimers,[26–30] micelles[31–35] or protein-bound complexes.[36–39]

In the past, the non-optimal water exchange rate has been a critical issue for macromolecular, Gd^{III}-based MRI contrast agents, since low exchange rates often limit proton relaxivity.[21,30] Nine-coordinate Gd^{III} poly(amino carboxylates) undergo a dissociative (**D**) or dissociative interchange ($\mathbf{I_d}$) water exchange process.[14] On the basis of structural considerations, recently we could accelerate the water exchange by inducing steric compression around the water binding site.[40,41] This was achieved by elongation of the amine backbone of the ligands by one CH_2 group, or by substituting one acetate arm by a propionate moiety. As a result, the water exchange rate increased remarkably for both linear and macrocyclic complexes ($k_{ex}^{298} = 150\times10^6\,s^{-1}$ and $270\times10^6\,s^{-1}$ for $[Gd(EPTPA\text{-}bz\text{-}NO_2)(H_2O)]^{2-}$ and $[Gd(TRITA\text{-}bz\text{-}NO_2)(H_2O)]^{-}$ vs $3.3\times10^6\,s^{-1}$ and $4.1\times10^6\,s^{-1}$ for $[Gd(DTPA)(H_2O)]^{2-}$ and $[Gd(DOTA)(H_2O)]^{-}$, respectively; DOTA = 1,4,7,10-tetra(carboxymethyl)-1,4,7,10-tetraazacyclododecane; DTPA = diethylenetriaminepentaacetic acid).

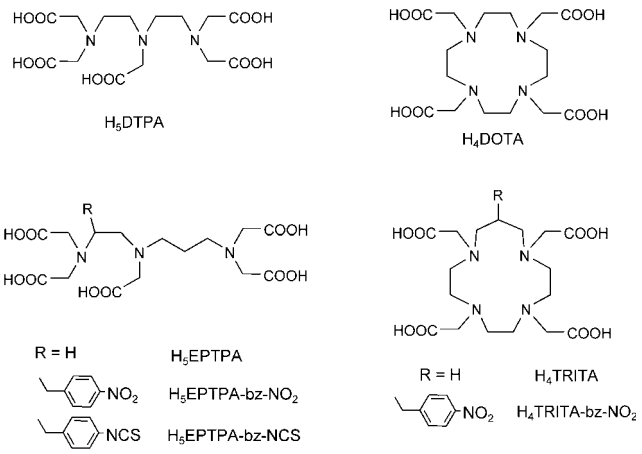

It has been previously demonstrated on various macromolecular systems, like dendrimers,[27,30] micelles[31,32] or polymers[21,22] that the coupling of a Gd^{III} chelate to a macromolecule does not significantly affect the rate and mechanism of the water exchange. It is also known from previous studies on dendrimeric Gd^{III} complexes, that slow water exchange was a limiting factor in attaining high relaxivity.[27,30] Consequently, the covalent linking of Gd^{III} chelates like $[Gd(EPTPA\text{-}bz\text{-}NO_2)(H_2O)]^{2-}$ with fast water exchange to a macromolecular system, such as a PAMAM dendrimer, could be an efficient way to increase relaxivity.

The noncomplexed Gd^{III} ion is toxic, thus it is administered in the form of metal chelates for contrast agent applications. In addition to the stability constant of the Gd^{III} complex under physiological conditions, the selectivity of the ligand for Gd^{3+} over endogenous metals, such as Zn^{2+} or Ca^{2+}, is a critical issue. In this respect, the EPTPA-bz-NO_2 ligand is preferred over the macrocyclic TRITA) ligand, since it is much more selective for Gd^{3+} over Zn^{2+} ($\log K_{GdL} = 19.20$, $\log K_{GdHL} = 3.40$, $\log K_{ZnL} = 16.01$, $\log K_{ZnHL} = 8.99$, $\log K_{ZnH2L} = 2.53$ for EPTPA-bz-NO_2[41] vs $\log K_{GdL} = 19.17$, $\log K_{GdHL} = 3.2$; $\log K_{ZnL} = 18.04$, $\log K_{ZnHL} = 4.57$ for TRITA[42,43]).

Here we report the synthesis of ethylenediamine-core PAMAM dendrimer[1] ligands of three different generations

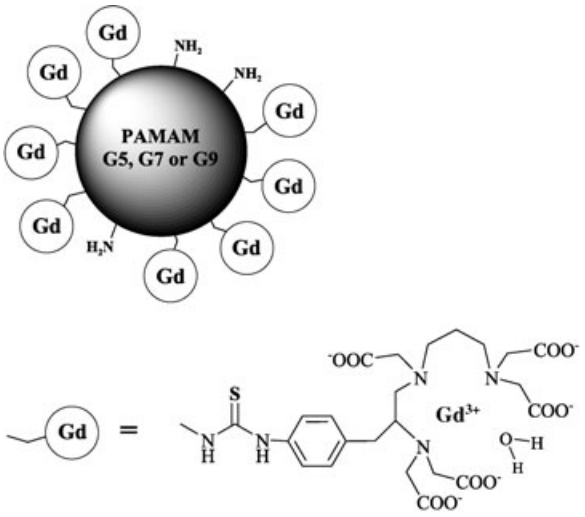

(5, 7 and 9) loaded with EPTPA chelators on the surface. Their Gd^{III} complexes [PAMAM-G5(N{CS}N-bz-Gd{EPTPA}$\{H_2O\}^{2-})_{111}$] (G5-$(GdEPTPA)_{111}$), [PAMAM-G7(N{CS}N-bz-Gd{EPTPA}$\{H_2O\}^{2-})_{253}$] (G7-$(GdEPTPA)_{253}$) and [PAMAM-G9(N{CS}N-bz-Gd{EPTPA}$\{H_2O\}^{2-})_{1157}$] (G9-$(GdEPTPA)_{1157}$) have been characterised with regard to potential MRI contrast agent applications. Water proton relaxivities have been measured for the different dendrimer generations at various Gd^{III} concentrations, Gd^{III}/chelate ratios and different ionic strengths. A pH-dependent relaxometric study has been performed on the three generations. Variable-magnetic-field ^{17}O longitudinal relaxation rates have been measured for G5-$(GdEPTPA)_{111}$ and its rotational dynamics (rigidity) has been described under acidic and basic conditions. In addition, ^{17}O transverse relaxation rates were used to determine the water exchange rate.

Results and Discussion

Synthesis of the dendrimeric chelates: We have covalently attached EPTPA chelate ligands through a benzyl-thiourea linkage to three generations (5, 7 and 9) of PAMAM dendrimers. These polymeric structures can carry a large number of chelating units on their surface. The EPTPA-bz-NCS ligand was prepared from (DL)-*p*-nitrophenylalanine in a multistep synthesis with an overall yield of 39%. In the last step, EPTPA-bz-NH_2[41,44,45] was reacted with $CSCl_2$ by using a standard two-phase methodology to give EPTPA-bz-NCS. The isothiocyanates are known to react very slowly with water, but are very reactive to amine groups. They were conjugated to the three amine-terminated PAMAM dendrimers. Due to the high affinity of the isothiocyanate toward amines, this type of conjugation is particularly well adapted for systems in which a large number of terminal groups have to react. Indeed, the same strategy has already been applied for the attachment of poly(amino carboxylates) to dendrimers.[26,28,29] Purification of the dendrimer–polychelates (before Gd incorporation) was achieved by ultrafiltration with appropriate molecular-weight cut-off filters.

The number of chelate groups linked to the dendrimer surface was assessed by complexometric titrations, elemental analysis and ^1H NMR spectroscopy. In the titration experiments, a solution containing the dendrimer was titrated by $GdCl_3$ (G5), $ZnCl_2$ (G7) and $CaCl_2$ (G9). This method allows us to determine the quantity of chelating unit per mass of dendrimer. The following values were obtained: $n_{EPTPA} = 1.077\times10^{-3}$, 7.301×10^{-4} and 8.846×10^{-4} mol g^{-1} for G5, G7 and G9, respectively. Based on the data obtained from the titration and the carbon content of the EPTPA-loaded dendrimer products determined by elemental analysis, one can calculate the average number of chelates per dendrimer molecule. (We consider that the carbon percentage is the most accurate among all elements (C, H, N, O, S) measured by elemental analysis; details are presented in the Supporting Information.) For the three different generations we obtain: G5-$(GdEPTPA)_{111}$, G7-$(GdEPTPA)_{253}$ and G9-$(GdEPTPA)_{1157}$ (Table 1). These values are in accordance with the average number of chelates per dendrimer estimated by ^1H NMR spectroscopy. Integration of the benzyl versus the alkyl region in the ^1H NMR spectrum indicated about 88% loading on G5-$(NH_2)_{128}$ and about 53% on G7-$(NH_2)_{512}$, while for the ninth-generation dendrimer the integration did not give reliable values. Elemental analysis and ^1H NMR spectroscopy are the two methods usually applied for the characterisation of poly(amino carboxylate)-loaded PAMAM dendrimers. The complexometric titration by itself cannot give the number of chelates per dendrimer molecule; however, it can be used to precisely determine the number of chelates per mass of the dendrimer product. In the preparation of all lanthanide-loaded samples, we used the chelate concentration determined in this way. In addition, a xylenol orange test was performed on each sample to check the absence of free Gd^{3+}, and the Gd^{3+} concentration was verified by ICP-AES measurements in all solutions.

Table 1. Number of terminal NH_2 groups and conjugated Gd^{III} chelates on the three different generations of dendrimers.

PAMAM generation	Number of terminal NH_2 groups	Number of Gd^{III} chelates	% of coupling
5	128	111	87
7	512	253	49
9	2048	1157	56

Gel-permeation chromatography on G5-$EPTPA_{111}$ showed a relatively narrow size distribution. Dynamic light-scattering measurements allowed us to estimate an average diameter of 8.0 nm for G5-$(GdEPTPA)_{111}$ (pH 6.7). This value compares well with that reported for a fifth-generation PAMAM dendrimer with an ammonia core and loaded with DO3A (DO3A = 1,4,7-tri(carboxymethyl)-1,4,7,10-tetraazacyclododecane) chelate ligands on the surface (7.8 nm measured in phosphate-buffered saline).[28]

Relaxivity studies

Relaxivity measurements at physiological pH: We have measured water proton relaxivities as a function of the Larmor frequency at variable temperatures (5, 25, 37 and 50 °C) for the three generations of dendrimers, that is, G5-$(GdEPTPA)_{111}$, G7-$(GdEPTPA)_{253}$ and G9-$(GdEPTPA)_{1157}$,

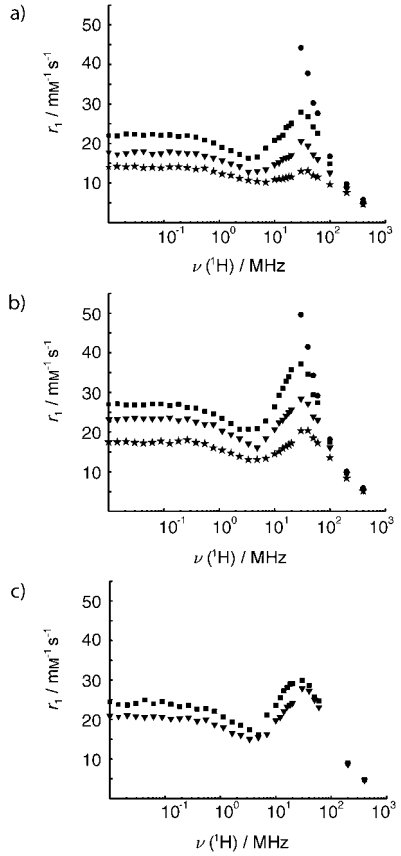

Figure 1. NMRD profiles of a) G5-$(GdEPTPA)_{111}$, b) G7-$(GdEPTPA)_{253}$ and c) G9-$(GdEPTPA)_{1157}$ at 5 °C (●) 25 °C (■), 37 °C (▼) and 50 °C (⋆), pH 7.4.

at physiological pH (7.4 in HEPES buffer; Figure 1; HEPES = 2-[4-(2-hydroxyethyl)-1-piperazinyl]ethanesulfonic acid). In all three cases, the slow rotation of the dendrimer leads to a high-field relaxivity peak, centred at 30–40 MHz, and typical of macromolecular systems. For all three dendrimer complexes, the relaxivities increase with decreasing temperature, and thus show the same temperature dependence as the monomeric $[Gd(EPTPA\text{-}bz\text{-}NO_2)(H_2O)]^{2-}$ complex.[41] This temperature dependence is the opposite to what has been previously reported in the literature for other dendrimer complexes, based on DOTA- or DTPA-type chelators. For instance, in the case of generation 5, 7, 9 and 10 PAMAM dendrimers bearing $[Gd(DOTA)(H_2O)]^-$ units on the surface, the relaxivity was found to increase with increasing temperature (for G = 7, $r_1 = 35\,mM^{-1}s^{-1}$ at 23 °C vs $40\,mM^{-1}s^{-1}$ at 37 °C; 20 MHz).[29] This was accounted for by the limiting effect of the slow water exchange. On G3,4,5-$[N(CS)\text{-}bz\text{-}Gd\text{-}(DO3A)(H_2O)]_{23,30,52}$ dendrimers, a variable-temperature ^{17}O NMR study experimentally proved the slow water exchange and that this slow exchange indeed limited the relaxivity gain brought by the slow tumbling.[27] The temperature dependence of r_1 for G5-$(GdEPTPA)_{111}$, G7-$(GdEPTPA)_{253}$ and G9-$(GdEPTPA)_{1157}$ implies that slow water exchange does not limit relaxivity.

The proton relaxivities increase from G5-$(GdEPTPA)_{111}$ to G7-$(GdEPTPA)_{253}$, and then they slightly decrease for G9-$(GdEPTPA)_{1157}$ at a given temperature (Figure 2). The

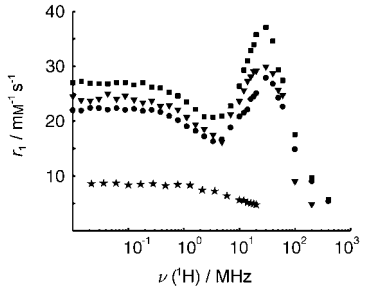

Figure 2. NMRD profiles of $[Gd(EPTPA\text{-}bz\text{-}NO_2)(H_2O)]^{2-}$ (pH 6.0; ⋆), G5-$(GdEPTPA)_{111}$ (●), G7-$(GdEPTPA)_{253}$ (■) and G9-$(GdEPTPA)_{1157}$ (▼) at 25 °C and pH 7.4.

Solomon–Bloembergen–Morgan theory predicts that after a certain limit, a further increase of the rotational correlation time no longer leads to a relaxivity gain. Thus, if the rotational correlation time is long enough on G7, no gain in relaxivity will be observed on going to G9. In this case, a small increase in the local flexibility of the Gd^{III} segments from G7 to G9 can cause a decrease in relaxivity. The NMRD (NMRD = nuclear magnetic relaxation dispersion) profiles of the G7 and G9 dendrimeric complexes have not been fitted, since clearly the Lipari–Szabo spectral functions, yielding local and global correlation times, would be needed for the analysis (see below); however, this analysis is very difficult and uncertain to perform without additional longitudinal ^{17}O relaxation rates. Consequently, we do not have exact data for the rotational correlation time on G7 and G9 and we cannot affirm whether the rotational correlation time is long enough not to influence relaxivity any more. Clearly, the global rotational correlation time is longer for G9 than for G7, given the larger molecular weight. The water exchange rate can be expected to be similar on both dendrimers. An eventual difference in the electronic relaxation cannot be excluded, but this point is difficult to judge. Consequently, it is the local motion of the Gd segments that can be mainly responsible for the slightly lower relaxivities of G9 versus G7. These results are in accordance with a variable generation study on G5,7,9,10-$[\{N(CS)\text{-}bz\text{-}Gd\text{-}(DOTA)\}^-]_{127,479,2041,3727}$ dendrimers in which the relaxivities first increased with generation then reached a plateau at G7.[29]

The relaxivities did not show concentration dependence for any of the generations (0.1–5 mM Gd^{3+} for G5-$(GdEPTPA)_{111}$ and G7-$(GdEPTPA)_{253}$; 0.1–1 mM Gd^{3+} for G9-$(GdEPTPA)_{1157}$; 40 MHz, 40 °C); neither were they dependent upon the sodium chloride concentration (0–1 M). These results point to the absence of aggregates in solution, which was independently confirmed by dynamic light-scattering measurements. The relaxivities also remained constant on varying the HEPES concentration (for G5-$(GdEPTPA)_{111}$, 2–450 equivalents of HEPES per Gd), indicating that the buffer does not interfere.

Dendrimers can have a high number of Gd^{III} chelates on the surface that can be relatively close to each other. Dipole–dipole interactions between electron spins of close Gd^{III} centres have been already observed by EPR or proton relaxometry for dinuclear[46] and trinuclear complexes,[47] micelles[48] and dendrimer complexes.[30] Such intramolecular Gd^{III}–Gd^{III} interactions lead to an increase in the electronic relaxation rate, which is unfavourable for relaxivity. Therefore one possibility to assess intramolecular dipole–dipole interactions is to measure the relaxivity as a function of the Gd^{III} "density" in the molecule. We have measured ^{1}H NMRD profiles for G5-$(GdEPTPA)_{111}$ and G7-$(GdEPTPA)_{257}$ with different Gd/EPTPA-chelating-unit ratios under physiological pH and 25 °C. As Figure 3 shows, at low frequencies the experimental relaxivities are different

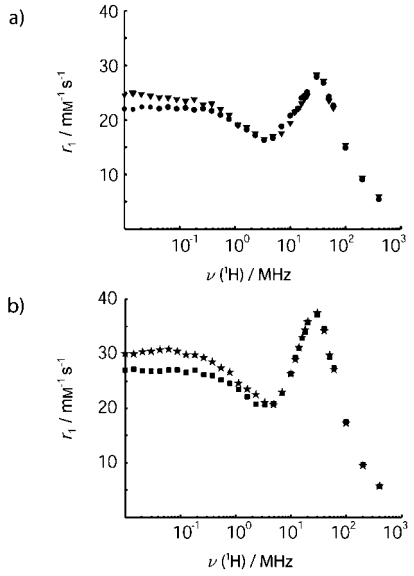

Figure 3. NMRD profiles of a) G5-$(GdEPTPA)_{111}$ with Gd^{III}/chelating ligand ratios of 1:1 (●) and 1:4 (▼) and b) G7-$(GdEPTPA)_{253}$ with a ratio of 1:1 (■) and 1:4 (⋆); 25 °C, pH 7.4.

for Gd/L ratios of 1:1 and 1:4, the relaxivity being higher for the 1:4 than for the 1:1 sample. Since at low magnetic fields the contribution of electronic relaxation dominates the relaxivities, this difference between the two samples indicates the presence of intramolecular dipole–dipole electron-spin interactions, which are evidently more important for the 1:1 than for the 1:4 sample. The intramolecular electron-spin interactions contribute to an increase in the electron-spin relaxation rate, and will consequently decrease proton relaxivity. On the other hand, at higher fields, in which the rotational contribution dominates and the electron-spin relaxation has practically no more effect on the relaxivity, identical r_1 values are measured for both samples. Similar observations were reported for micellar systems with variable Gd^{III} loading.[48]

We have also measured proton relaxivities for the three generations of dendrimers as a function of pH between pH 6 and 12 (40 MHz, 40 °C; Figure 4). Below pH 6, the

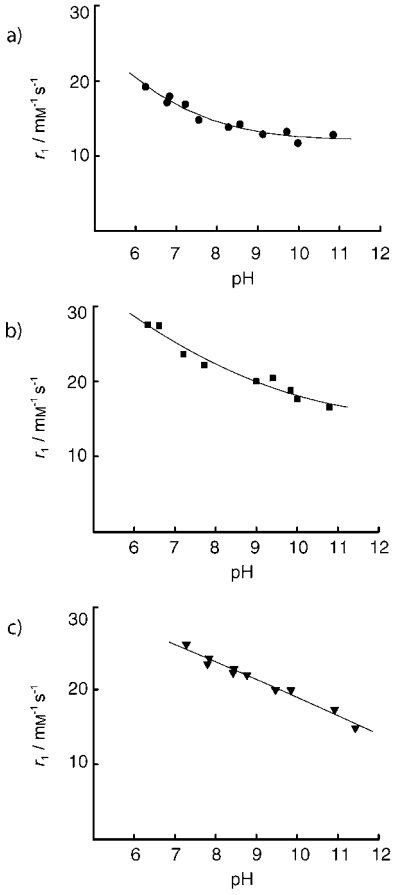

Figure 4. The pH-dependent ^{1}H relaxivities for a) G5-$(GdEPTPA)_{111}$, b) G7-$(GdEPTPA)_{253}$ and c) G9-$(GdEPTPA)_{1157}$ at 40 MHz and 40 °C. The tendency lines represent a polynomial fit to guide the eyes.

dendrimer complexes are not soluble, probably due to the protonation of the amino functions in the skeleton. For all generations, the relaxivity increases with decreasing pH and this variation is fully reversible. For solubility reasons, a more detailed study on the influence of pH was performed only on the fifth-generation dendrimer, G5-$(GdEPTPA)_{111}$.

Variable pH studies on G5-$(GdEPTPA)_{115}$—UV-visible spectrophotometry: To learn about the hydration state of G5-

$(LnEPTPA)_{111}$ complexes, and particularly its eventual variation with pH, we performed a pH-dependent UV-visible study on aqueous solutions of the Eu^{III} analogue at 298 K. The $^7F_0$–$^5D_0$ transition band of Eu^{III} (575.0–585 nm) is very sensitive to the coordination environment and is often used to test the presence of differently coordinated species.[49] The G5-$(EuEPTPA)_{111}$ complex at both pH 9.9 and 6.4 has a single absorption band in this region that proves the absence of a hydration equilibrium in solution. The same result was found for the corresponding monomer EuEPTPA complex.[41] Moreover, the maximum of the absorption band is identical for the acidic and basic samples; this proves the similarity of the coordination environment at the two different pHs. By analogy, we assume that the same hydration mode (no hydration equilibrium) exists for the corresponding Gd^{III} complex as well.

Variable pH studies on G5-$(GdEPTPA)_{115}$—^{17}O NMR and ^1H NMRD spectroscopy: As Figure 4 shows, the proton relaxivities are strongly dependent on pH; from pH 11 to 6, r_1 increases by about 60% for all the three generations. Such pH dependence can result from the pH dependence of the water exchange rate or of the rotational correlation time, the two main influencing factors for proton relaxivity at high fields. To gain more insight into the pH behaviour of these parameters, we performed a variable-temperature ^{17}O NMR study on G5-$(GdEPTPA)_{111}$ under both basic and acidic conditions, at pH 9.9 and 6.0 (the most acidic medium at which the dendrimer is still soluble). Transverse and longitudinal ^{17}O relaxation rates were measured at two different magnetic fields (4.7 and 9.4 T); multiple fields are indispensable for a detailed description of the rotational dynamics. The ^{17}O relaxation data are presented in Figure 5 for the two different pHs.

In the ^{17}O NMR measurements, a solution of G5-$(YEPTPA)_{111}$ was used as external reference, at the same concentration and pH as the Gd^{III} sample. Previous studies on low-molecular-weight Gd^{III} complexes at pH~5 have shown that acidified water or the corresponding Y^{III} complex can be alternatively used as diamagnetic reference (the difference in the measured T_1 and T_2 was within the experimental error). For the dendrimer G5-$(YEPTPA)_{111}$ complex, however, both the longitudinal and transverse diamagnetic relaxation rates were found to be considerably lower (~30–50%) than for acidified water. Therefore, in all measurements, the Y^{III} complex was used as diamagnetic reference.

The reduced ^{17}O longitudinal relaxation rate of an aqueous solution of Gd^{III} is determined by quadrupolar and dipolar relaxation mechanisms, both dependent on the rotation of the Gd-coordinated water oxygen vector. A comparison of the $\ln(1/T_{1r})$ values in Figure 5 clearly shows that the pH has a significant influence on the rotational dynamics. Moreover, the ^{17}O longitudinal relaxation rates at both pHs also depend on the magnetic field, which is characteristic of slowly rotating systems. In such a case, the usual Solomon–Bloembergen spectral density functions cannot describe the experimental ^{17}O $\ln(1/T_{1r})$ data. Recently, the model-free Lipari–Szabo approach, commonly used for the description of motional dynamics of proteins, oligosaccharides, and so forth,[50,51] was adapted to paramagnetic ^{17}O longitudinal relaxation.[21] This approach was successfully used to characterise rotation of different macromolecular Gd^{III} complexes, like linear polymers,[21,23] micellar systems[32] or dendrimers.[30] In several cases, proton relaxivities were also included in the analysis and fitted simultaneously with the ^{17}O data. The spectral density functions applied in the Lipari–Szabo analysis involve a global rotational correlation time (τ_g), which can be attributed to the global movement of the macromolecule, and a local rotational correlation time (τ_l), which describes the local movement of the Gd segments within the macromolecule. The degree of spatial restriction of the local motion with regard to the global rotation is given by an additional model free parameter (S^2). For a totally free internal motion $S^2=0$, while for a local motion that is exclusively correlated to the global motion, $S^2=1$.

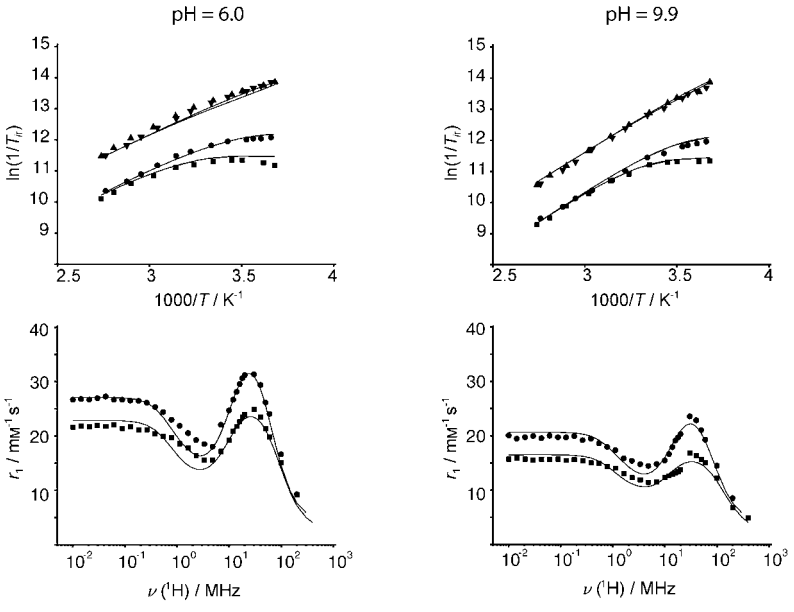

Figure 5. Top: Variable-temperature, reduced longitudinal and transverse ^{17}O relaxation rates for G5-$(GdEPTPA)_{111}$ at pH 6.0 (left) and 9.9 (right) $B=9.4$ T ($\ln(1/T_{1r})$:■; ($\ln(1/T_{2r})$: ▲) and 4.7 T ($\ln(1/T_{1r})$ ●; ($\ln(1/T_{2r})$: ▼). Bottom: ^1H NMRD profiles at 25 °C (●) and 37 °C (■). The lines represent the curves fitted to the experimental points. The reduced longitudinal and transverse ^{17}O relaxation rates are calculated from the observed rates $1/T_{1,2}$ by taking into account the diamagnetic relaxation rates $1/T_{1,2A}$ and the molar fraction of the coordinated water, P_m: $1/T_{1,2r}=1/P_m[(1/T_{1,2})-(1/T_{1,2A})]$.

The variable-temperature, multiple-field ^{17}O longitudinal and reduced transverse relaxation rates and the proton relaxivities for G5-$(GdEPTPA)_{111}$ have been fitted simultaneously for each sample (pH 6.0 and 9.9). In the fit, we did not include chemical shifts, which we generally use as a direct measure of the scalar coupling constant, $A/\hbar$. Given the relatively low concentration of the ^{17}O NMR samples, the shifts could not be obtained with a sufficient precision; therefore we did not use them in the analysis. Instead, the value of the coupling constant was fixed in the analysis to -3.2×10^6 rad s^{-1}, obtained previously for the monomer $[Gd(EPTPA\text{-}bz\text{-}NO_2)(H_2O)]^{2-}$ complex.[41] Although of low quality, the similar values of the chemical shifts measured at pH 6.0 and 9.9 also point to a similar hydration state of the Gd^{III}, as it was evidenced for the Eu^{III} analogue by the UV-visible study.

The electron-spin relaxation has been described as in the conventional Solomon–Bloembergen–Morgan (SBM) theory.[14] It takes into account only the transient zero-field-splitting (ZFS; modulated by vibration, intramolecular rearrangement and collision with water molecules). In the past years it has become evident that this theory cannot provide an appropriate description of the electronic relaxation of Gd^{III} complexes. It has been shown that an additional contribution of static ZFS (modulated by molecular reorientation of the complex) has also to be considered.[52–54] Moreover, for macromolecular systems the Redfield relaxation theory describing the time dependence of the correlation functions of the spins system components is not valid, thus the theory developed for low-molecular-weight complexes[53,54] cannot be used for macromolecular chelates. Consequently, the electronic relaxation parameters as obtained in our analysis (correlation time for the modulation of the ZFS, τ_v, the trace of the square of the zero-field-splitting tensor, Δ^2) are only fitting parameters and should not be interpreted in terms of real physical meaning. The failure of the SBM equations to describe electronic relaxation is manifested in the deviations between calculated and observed proton relaxivites around the relaxivity minimum of the NMRD curve, for which the electronic contribution is significant (0.8–4 MHz). At higher fields, the relaxivity is dominated by the rotational correlation time. It is important to note that the approximation by using the Solomon–Bloembergen–Morgan approach to describe electronic relaxation will not lead to incorrect rotational correlation times, since the rotation is essentially determined by the high-field proton relaxivities (for which the effect of electronic relaxation is negligible) and by the ^{17}O longitudinal relaxation rates, which are not influenced by electronic relaxation. In other words, even if the calculated NMRD profiles do not fit exactly the experimental data at intermediate fields, the parameters characterising the rotation are well defined.

To gain more insight into electron-spin relaxation, we have also recorded EPR spectra of G5-$(GdEPTPA)_{111}$ at X- and Q-band. However, due to the lack of an appropriate theory for macromolecular Gd^{III} complexes, these results have not been included in the fit of the ^{17}O NMR and NMRD data and are only used to draw qualitative conclusions. The transverse electronic relaxation rates are about 40% higher for G5-$(GdEPTPA)_{111}$ than for the monomer $[Gd(EPTPA\text{-}bz\text{-}NO_2)(H_2O)]^{2-}$ at the same temperature and magnetic field ($1/T_{2e}=6.9\times10^9$ s^{-1} vs 4.7×10^9 s^{-1}, respectively; at X-band; pH 6.0, 25 °C). This is in accordance with previous results showing that electronic relaxation rates are higher on macromolecular chelates than on the corresponding monomers, and they increase with increasing size within a family of analogous macromolecules.[21] The increase in the electron-spin relaxation rate can originate from a contribution of the dipole–dipole intramolecular interactions between close Gd^{III} centres as discussed above, but also from the static ZFS, which is dependent on the rotational dynamics. Moreover, the peak-to-peak EPR linewidths, ΔH_{pp}, measured for the dendrimer complex, change with pH. They are about 10–15% larger under acidic than under basic conditions, which means that electronic relaxation is faster at lower pH.

Given the large number of parameters involved in the analysis of the ^{17}O NMR and NMRD data, some of them had to be fixed to common and physically meaningful values. The diffusion constant, D^{298}_{GdH}, and its activation energy, E_{DGdH}, were fixed to 20×10^{-10} m^2 s^{-1} and 25 kJ mol^{-1}, respectively.[55] For the distances we used $r_{GdO}=2.5$ Å (Gd electron spin and ^{17}O nucleus distance), $r_{GdH}=3.1$ Å (Gd electron spin and ^1H nucleus distance) and $a_{GdH}=3.5$ Å (closest approach of the bulk water molecules). The quadrupolar coupling constant for the bound water oxygen atoms, $\chi(1+\eta^2/3)^{1/2}$, was fixed to 5.2 MHz.[56] The longitudinal ^{17}O relaxation is related to motions of the Gd-coordinated water oxygen vector, while the proton relaxation is determined by motions of the Gd-coordinated water proton vector. For the ratio of the rotational correlation time of the Gd–H_{water} and Gd–O_{water} vectors, τ_{RH}/τ_{RO}, similar values have been found for various low-molecular-weight monohydrated Gd^{III} complexes, both by experimental studies and MD simulations ($\tau_{RH}/\tau_{RO}=0.65\pm0.2$).[56,57] This τ_{RH}/τ_{RO} ratio, within the given error, is considered as a general value for the ratio of the two rotational correlation times. In the simultaneous analysis of ^{17}O NMR and NMRD data for the dendrimer complex, we fixed the ratio of the local correlation times of the Gd-coordinated water proton vector (τ_{lH}) and the Gd-coordinated water oxygen vector (τ_{lO}) to 0.65. The global rotational correlation times obtained from oxygen and proton relaxation are identical ($\tau_{gO}=\tau_{gH}$). In the analysis, we fitted the rotational correlation times τ^{298}_{lO} and τ^{298}_{gO} characterizing the motion of the Gd–O_{water} vector. The experimental ^{17}O NMR and NMRD data and the fitted curves for G5-$(GdEPTPA)_{111}$ at pH 6.0 and 9.9 are presented in Figure 5. The relevant parameters obtained in the fit are shown in Table 2. For the electronic relaxation parameters we obtained the following values: $\tau^{298}_v=37$ and 30 ps; $\Delta^2=0.06$ and 0.1×10^{20} s^{-2} for pH 6.0 and 9.9, respectively; E_v was fixed to 1.0 kJ mol^{-1}. All equations used in the fit are given in the Supporting Information.

Table 2. Parameters obtained for G5-(GdEPTPA)$_{111}$ chelates at pH 6.0 and 9.9 from the simultaneous analysis of ^{17}O NMR and NMRD data.

	pH 6.0	pH 9.9
k_{ex}^{298} [10^6 s^{-1}]	150 ± 30	180 ± 30
$\Delta H^{\neq}$ [kJ mol^{-1}]	20.0 ± 4	27.9 ± 4
$\Delta S^{\neq}$ [J mol^{-1} K^{-1}]	−21 ± 12	4 ± 12
τ_{gO}^{298} [ps]	4040 ± 300	2950 ± 250
E_{gO} [kJ mol^{-1}]	25 ± 2	32 ± 3
τ_{iO}^{298} [ps]	150 ± 15	125 ± 13
E_{iO} [kJ mol^{-1}]	31 ± 3	37 ± 3
S^2	0.43 ± 0.03	0.36 ± 0.03

Water exchange: The water exchange rates calculated for the two pHs are very close (within 20%) and are also similar to that obtained for the corresponding monomer [Gd(EPTPA-bz-NO$_2$)(H$_2$O)]$^{2-}$ ($k_{ex}^{298} = 150 \times 10^6$ s^{-1}).[41] Consequently, the gain in accelerating water exchange by steric crowding around the bound water is not reduced by attachment of the chelate to the macromolecular entity. This is another piece of evidence that adds up to previous observations showing that covalent coupling of Gd^{III} chelates to macromolecules does not significantly change the rate and mechanism of water exchange.[21–23,27,30] The similarity of the k_{ex} values at pH 6.0 and 9.9 indicates that in this pH range there is no chemical or structural change in the close environment of the bound water. Many preceding studies have shown that water exchange is influenced exclusively by changes in the inner coordination sphere of the Gd^{III}.

The proton relaxivity is determined by the proton exchange rate, which, for the typical Gd^{III}–poly(amino carboxylates) around physiological pH, is equal to the water exchange rate. Proton exchange can be accelerated by H$^+$ or OH$^-$ catalysis. This results in an increase of the proton relaxivities at high and low pH values. In the case of the closely related [Gd(DTPA)(H$_2$O)]$^{2-}$, the relaxivity starts to increase only above pH ~ 13 as a sign of the increased proton exchange rate originating from the OH$^-$ catalysis.[58] For the G5-(GdEPTPA)$_{111}$ the proton exchange rate very likely remains unchanged between the two pHs studied (6.0 and 9.9), and equals the water exchange rate.

Rotation: The ultimate objective of this study was to describe in detail the rotational dynamics of the dendrimer complex, and in particular, to determine if the pH dependency of the proton relaxivities can be related to a pH-dependent rotational dynamics. We have seen above that neither the hydration state of the dendrimer complex, nor the exchange rate of the coordinated water changes with pH. Moreover, a complete ^{17}O NMR study (T_1 and T_2) has also been performed on [Gd(EPTPA)(H$_2$O)]$^{2-}$, the monomer Gd^{III} unit of G5-(GdEPTPA)$_{111}$ at pH 6.0 and 9.9. The reduced longitudinal and transverse ^{17}O relaxation rates showed no dependence on pH (all data are presented in the Supporting Information). These results are also in accordance with previous potentiometric titrations, which proved that above pH 5 only the species [Gd(EPTPA)(H$_2$O)]$^{2-}$ or [Gd(EPTPA-bz-NO$_2$)(H$_2$O)]$^{2-}$ are present in solution (below this pH, a protonated GdHL species also exists).[41] The pH-invariant behaviour of the monomeric complex clearly indicates that the pH effect observed on the longitudinal proton and ^{17}O relaxation rate of the dendrimer complexes originates from the PAMAM skeleton.

For G5-(GdEPTPA)$_{111}$ under both acidic and basic conditions, the model-free Lipari–Szabo approach describes reasonably well the experimental ^{17}O and ^{1}H longitudinal relaxation rates, the data that are influenced by the rotational dynamics (Figure 5). The local correlation times for both samples are considerably shorter than the global ones; this indicates an important flexibility of the Gd^{III} segments. It clearly shows that the motion of the Gd^{III} chelates on the surface of the dendrimer does not take full advantage of the slow rotation of the macromolecular assembly. This flexibility seems to be more pronounced for PAMAM dendrimers than for Gadomer 17,[30] in which both the local rotational correlation time and the S^2 parameter were found to be greater relative to G5-(GdEPTPA)$_{111}$ (Table 3). Gadomer 17 is a poly-lysine-based dendrimer with a trimesoyltriamide central core and 24 Gd(DO3A)-monoamide chelates on the surface. On G5-(GdEPTPA)$_{111}$ the local motion of the Gd^{III} segments shows little dependence on pH as demonstrated by the similar τ_{iO}^{298} values obtained at pH 6.0 and 9.9. In contrast to the local motions, the overall tumbling is strongly pH dependent; the global rotational correlation time of the dendrimer complex increases remarkably (37%) from pH 9.9 to pH 6.0. Moreover, the complex is slightly more

Table 3. Comparison of water exchange rates, rotational parameters and relaxivities for various macromolecular systems analysed with the model-free Lipari-Szabo approach.

	k_{ex}^{298} [$\times 10^6$ s^{-1}]	τ_g^{298} [ps]	τ_i^{298} [ps]	S^2	r_1 [mM^{-1} s^{-1}] (20 MHz 37 °C)	Ref.
dendrimers						
Gadomer 17	1.0	3050	760	0.50	17.18	[30]
G5-(GdEPTPA)$_{111}$ (pH 6.0)	150	4040	150	0.43	23.9	this work
G5-(GdEPTPA)$_{111}$ (pH 9.9)	180	2950	125	0.36	13.7	this work
linear polymers						
[Gd(DTPA-BA)(CH$_2$)$_{10}$(H$_2$O)]	0.66	2900	490	0.35	15.38[a]	[21]
[Gd(DTPA-BA)(CH$_2$)$_{12}$(H$_2$O)]	0.50	4400	480	0.35	19.55[a]	[21]
[Gd(EGTA-BA)(CH$_2$)$_{12}$(H$_2$O)]	2.2	3880	321	0.25	12.60[a]	[23]
micelles						
[Gd(DOTAC12)(H$_2$O)]$^-$	4.8	1600	430	0.23	17.20[b]	[32]
[Gd(DOTAC14)(H$_2$O)]$^-$	4.8	2220	820	0.17	17.83	[32]
[Gd(DOTASAC18)(H$_2$O)]$^-$	4.8	2810	330	0.28	15.63[c]	[32]

[a] 35 °C. [b] 25 °C. [c] 18 MHz.

rigid under acidic conditions, reflected by a higher S^2. Therefore, the higher relaxivity measured in acidic solution can be related essentially to a higher global rotational correlation time, τ_{gO}, and order parameter, S^2.

The Q-band EPR measurements also seem to support the slower rotation at acidic rather than basic pH. The peak-to-peak linewidth is larger at lower pH (see above), which can be attributed to a more important contribution of the static ZFS, induced by a slower rotation.

The difference in τ_{gO} between the two pH values suggests that the overall size of the dendrimer becomes larger when the internal amine groups get protonated. This is reasonable, since the protonation of the amine nitrogen atoms creates positive charges that will lead to an increasingly important repulsion inside the dendrimer. The influence of pH on the structure of dendrimers has been previously investigated by various techniques. Monte Carlo simulations have demonstrated that the density profiles of dendrimeric polyelectrolytes are tuneable between a dense core at low pH to a dense shell at high pH.[59,60] Molecular dynamics simulations of PAMAM dendrimers have been also performed at varying pH from the second- to sixth-generations.[61] They have shown globular and loosely compact structures at high pH (>10), in contrast to highly ordered, and extended structures at low pH (<4). These results were correlated to the fraction of protonated tertiary amine groups. For a PAMAM-G5 dendrimer without any surface substituent these fractions are 0.99 (pH 5), 0.42 (pH 7), and 0.007 (pH 9).[62] At low pH (<5), the protonation of the tertiary amine groups fills the whole dendritic interior with cations, and the strong charge–charge repulsion makes the structure more expanded.

At the more acidic pH of our study (pH 6.0), a large fraction of the tertiary amine groups is protonated, thus one observes slower global motions due to the extended dendrimeric structure. On increasing the pH, the amine groups gradually deprotonate, the positive charges disappear and there is no more repulsing force in the interior of the dendrimer. This leads to shrinkage and continuous decrease of the global rotational correlation time all along the pH range at which deprotonation occurs. Due to the presence of a high number of protonatable tertiary amines, dendrimers behave like polyelectrolytes, implying that protonation covers a much larger pH interval than in the case of an individual protonation site. Thus the rotational correlation time and consequently the proton relaxivity is continuously changing over a wide pH range, as it is indeed observed for all three generation dendrimer complexes (Figure 4). Moreover, since the number of tertiary amine protonating sites increases with increasing dendrimer generation, the pH range in which protonation continuously occurs also becomes more and more extended for higher generations. As a consequence, the relaxivity change brought by the changing rotational correlation time will also cover a more extended pH range, as is observed. Figure 4 demonstrates that the relaxivity becomes constant above pH ~9 for G5-$(GdEPTPA)_{111}$, around pH 10 for G7-$(GdEPTPA)_{253}$, while it is still strongly decreasing at pH >11 for G9-GdEPTPA$_{1157}$.

The gradual protonation of the internal tertiary amines in the dendrimer also has an effect on hydrogen-bond formation, which can in turn influence the rigidity. The S^2 parameter is slightly higher for the lower pH sample (pH 6.0) than for the basic one (pH 9.9); this fact supports the hypothesis that hydrogen bonding is more important in the acidic sample.

It has to be noted that the protonation of the internal amines of the dendrimer skeleton increases the number of exchangeable protons. This can lead to an additional ("second sphere") relaxation effect, thus contributing to an increased relaxivity. The analysis of the pH-dependent ^{17}O longitudinal relaxation rates clearly showed that the pH changes influence the rotational dynamics, and the simultaneous fit of the ^{17}O and ^{1}H relaxation rates could well describe the experimental data, without considering any second sphere effect. An eventual "second sphere" contribution to the overall proton relaxivity is very difficult to describe theoretically, since we have no information of the number of protons involved, of their distance from the paramagnetic centre and so forth. Moreover, these protons on the dendrimer skeleton are relatively far from the Gd^{III} ions and this minimises the importance of this relaxation effect. Consequently, we did not include "second sphere" contributions in our analysis. Taking the good fit of the experimental data with our model, it appears to be a reasonable assumption.

It is somewhat surprising that relatively low values are obtained for the local rotational correlation times; they are about the double of the τ_{RO} value calculated for the motion of the Gd-coordinated water oxygen vector of the monomer GdEPTPA chelate (75 ps). These τ_{lO}^{298} values are particularly low relative to that reported for Gadomer 17 (Table 3). However, the structure of Gadomer 17 is considerably different. In particular, the macrocycles are conjugated to the dendrimer through two, successive amide bonds with a CH_2 unit in between. Amide groups are planar and do not allow for free rotation, so the CH_2 linker between the amides is the single point that brings some degree of freedom in the local motion of the Gd chelate. As a consequence, Gadomer 17 has much more restricted local motions and a remarkable rigidity as given by the high value of the S^2 parameter relative to the other macromolecular systems analysed by the Lipari–Szabo approach.

The τ_{l}^{298} values published for different linear copolymer chelates were higher as well (Table 3).[21,23] In these polymers, the chain consists of alternating Gd^{III} poly(amino carboxylate) and $(CH_2)_x$ segments. Here each of the Gd^{III} chelates has two points of attachment to the macromolecule that can contribute to a slower local motion of the Gd-coordinated water oxygen vector. In the case of the PAMAM dendrimers, there is a single point of attachment, thus the local motions are less restricted relative to the linear copolymers, manifested by the lower local rotational correlation times.

Previously, the Lipari–Szabo spectral density functions have been also used to analyse the rotational dynamics of various micellar Gd^{III} complexes.[32] In these systems, the macrocyclic Gd^{III} complex contained a long hydrocarbon chain, attached either directly or through a $-CH_2-$amide function to an acetate arm of the DOTA chelator. The local rotational correlation times were found to depend on both the length and the linking mode of the hydrocarbon chain to the ligand. Namely, the direct attachment of the long chain to the acetate carbon resulted in considerably longer local rotational correlation times than the amide coupling. Since for these micelles the rigidity is given by the hydrophobic interactions between the hydrocarbon chains, it is clear that an additional amide group inserted between the Gd^{III} complex and the hydrophobic chain will increase the mobility of the Gd^{III} units. This was the first study that experimentally proved the importance of the linker structure in ensuring slow local motions in macromolecular Gd^{III} complexes.

In the case of our dendrimer complexes, the linker consists of a highly flexible CH_2 group connected to the aromatic and rigid phenyl group and then the thiocyanate function binds directly to the dendrimer. Due to the convenient synthesis and the stability, this benzylisothiocyanate linker is probably the most widely used to couple poly(amino carboxylate) complexes to various macromolecules for radiopharmaceutical or MRI contrast agent purposes. Unfortunately, it seems that, with regard to rigidity, it is not the best choice for the construction of macromolecular MRI contrast agents, in which it is essential to eliminate all points of flexibility in coupling the Gd^{III} chelate to the macromolecule.

Limiting factors for proton relaxivity of the dendrimer complex: Until now the slow water exchange was a critical issue for dendrimeric Gd^{III} chelates as potential MRI contrast agents. When proton relaxivities increase with temperature, slow water exchange is always a limiting factor. In comparison to previously reported dendrimer-based Gd^{III} complexes, the relaxivities measured for G5-$(GdEPTPA)_{111}$, G7-$(GdEPTPA)_{253}$ or G9-$(GdEPTPA)_{1157}$ are not spectacularly higher (Table 4), though the water exchange is much faster. The optimal range of the water exchange rate to attain maximum relaxivities is relatively restricted; moreover it might also depend on the magnetic field and on the actual value of the other influencing parameters. It has to be noted that if the relaxivity is limited by a faster than optimal water exchange rate, the temperature dependence will be the same as for a limitation by fast rotation, that is, the relaxivities increase with decreasing temperature.

The water exchange rate for the dendrimer G5-$(GdEPTPA)_{111}$ complex is $k_{ex}^{298}=150\times10^6\,s^{-1}$ (pH 6.0). We have simulated proton relaxivity profiles by using the parameters obtained for G5-$(GdEPTPA)_{111}$, except for the water exchange rate, which was varied between 5–150 $\times$ $10^6\,s^{-1}$ (Figure 6a). The maximum relaxivities attained at the high field peak of the profile show that the actual water exchange rate is faster than the optimal value ($\sim35\times10^6\,s^{-1}$), for which the highest relaxivities are calculated. However, the gain in relaxivity would not be enormous (15%) even with an optimal water exchange rate either, since the relaxivity is mainly limited by the fast local rotation and low rigidity of the dendrimer. This is nicely demonstrated by Figure 6b which presents simulated relaxivity curves for varying values of the S^2 parameter, with all other parameters kept constant at values calculated for G5-$(GdEPTPA)_{111}$. The relaxivity gain that could be realised by freezing out the local motion of the Gd^{III} chelates on the den-

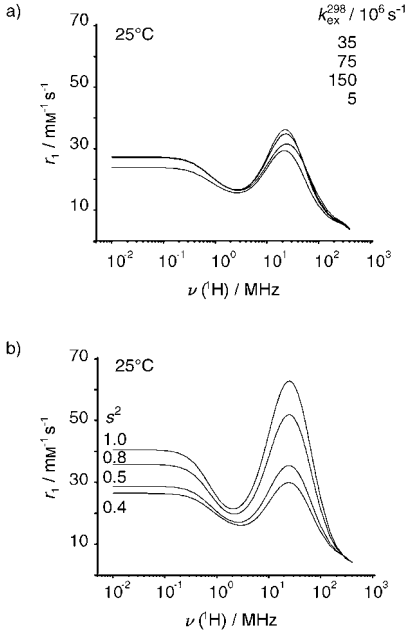

Figure 6. Simulated proton relaxivities as a function a) of the water exchange rate, k_{ex}^{298} and b) of the general order parameter S^2 for G5-$(GdEPTPA)_{111}$ (pH 6.0; 25 °C).

Table 4. Comparison of relaxivities (20 MHz) for different dendrimeric Gd^{III} complexes.

	T [°C]	r_1 [mM^{-1} s^{-1}]	Ref.
Gadomer[a]	25/37	16.5/17.2	[30]
[G5((N{CS}-bz-Gd-(DOTA)$(H_2O))^-_{96}$]	23	30	[29]
[G7((N{CS}-bz-Gd-(DOTA)$(H_2O))^-_{380}$]	23	35	[29]
[G9((N{CS}-bz-Gd-(DOTA)$(H_2O))^-_{1320}$]	23	36	[29]
[G3((N{CS}-bz-Gd-(DO3A)$(H_2O))_{23}$]	37	14.6	[27]
[G4(N{CS}-bz-Gd-(DO3A)$(H_2O))_{30}$]	37	15.9	[27]
[G5((N{CS}-bz-Gd-(DO3A)$(H_2O))_{52}$]	37	18.7	[27]
[G2((N{CS}-bz-Gd-(DTPA)$(H_2O))^{2-}_{11}$][b]	20	21.3	[26]
[G6((N{CS}-bz-Gd-(DTPA)$(H_2O))^{2-}_{170}$][b]	20	34.0	[26]
G5-$(GdEPTPA)_{111}$	25/37	25.1/17.1	this work
G7-$(GdEPTPA)_{253}$	25/37	35.8/25.6	this work
G9-$(GdEPTPA)_{1157}$	25/37	29.2/24.2	this work

[a] pH 6.0. [b] 25 MHz.

drimer surface ($S^2=1$) is over 100%.

In the early development of contrast agents, it seemed easier to slow down rotation of Gd^{III} chelates by applying macromolecular systems than to optimise their water/proton exchange rate. Now it has become clear that the water exchange rate can be tuned to a desired value, but it is not evident which macromolecular systems have sufficiently high internal rigidity. Rotational dynamics have been characterised in detail, usually by the Lipari–Szabo approach, only for a limited number of macromolecular systems (dendrimers, micellar systems and linear polymers). The majority the common macromolecules evoked in the context of MRI contrast agents do not have sufficient rigidity. Clearly, new, innovative systems are needed to make a revolutionary step in the development of high-relaxivity MRI contrast agents. We have recently shown that self-assemblies based on heterodi- or heterotritopic ligands can present extreme rigidity.[63,64] Nevertheless, dendrimers will always have a great potential in targeting or as contrast agents for simultaneous use in different diagnostic techniques (infrared imaging, luminescence, etc.). They have the advantage of possessing a very large number of easily derivatisable sites on the surface that can be loaded with various functions in addition to the paramagnetic complexes. These functions can be targeting vectors or reporters in other diagnostic techniques. Moreover, dendrimers can be obtained in a relatively uniform size, which is always an advantage in biomedical applications.

Conclusion

Three different generations (5, 7 and 9) of PAMAM dendrimers have been loaded with EPTPA, a chelate that ensures fast water exchange with a Gd^{III} complex. The dendrimeric Gd^{III} complexes were characterised with regard to MRI contrast agent applications by proton relaxivity and ^{17}O NMR studies. Their proton relaxivity shows an important pH-dependency, which is related to the pH-dependent rotational dynamics. The rotational dynamics of the G5-$(GdEPTPA)_{111}$ dendrimer were described under acidic and basic conditions by using the Lipari–Szabo spectral density functions. The correlation time of the global motion remarkably increases with decreasing pH. This is a consequence of the gradual protonation of the tertiary amines inside the dendrimer which, through the increasing repulsion between the positively charged nitrogen atoms, leads to an extended structure and thus a slower global rotation. Hydrogen bonding also becomes more important at lower pH, contributing to the rigidity of the macromolecule. However, the local motions of the Gd^{III} segments on the surface are too rapid and strongly limit the proton relaxivity.

Although this is the first time that such pH-dependency of the proton relaxivity is reported for dendrimeric Gd^{III} complexes, it is very likely a general phenomenon for dendrimers with a PAMAM scaffold.

Experimental Section

All reagents and solvents were commercially available. EPTPA-bz-NH_2 was obtained as described in the literature.[41,45] The ethylenediamine core PAMAM dendrimers with primary amines on the surface G5-$(NH_2)_{128}$, G7-$(NH_2)_{512}$ and G9-$(NH_2)_{2048}$ were purchased as aqueous solutions from Dendritech Inc. (Midland, MI). Ultrafiltration membranes YM10 and YM30 were obtained from Amicon, (Bedford, MA). ^1H NMR spectra were recorded on a Bruker DPX-400 spectrometer in D_2O. Elemental analysis was performed by Analytische Laboratorien (Lindlar, Germany). Gel-permeation chromatography was done by Polymer Standards Service GmbH (Mainz, Germany).

Synthesis of EPTPA-bz-NCS: HCl (3 M, 13 mL), CCl_4 (6 mL) and $CSCl_2$ (3.6 mL, 47 mmol) were added to a flask containing EPTPA-bz-NH_2 (1.94 g, 2 mmol). The resulting orange-red biphasic solution was protected from light and stirred at room temperature for 5 h. The reaction mixture was then evaporated to dryness and dried under vacuum at 40 °C for 4 h to give a pale yellow solid (1.35 g, quantitative). ^1H NMR (400 MHz, D_2O [HDO] = 4.80 ppm): $\delta = 2.20$ (m, 2H), 2.74 (dd, $J = 7.8$ Hz, $J = 8.0$ Hz, 1H), 3.12 (dd, $J = 6.5$ Hz, $J = 6.4$ Hz, 1H), 3.56–3.68 (m, 11H), 4.02 (s, 1H), 4.06 (s, 5H), 7.35 ppm (s, 4H); MS (ESI): m/z: 555.6 $[M+H]^+$.

Synthesis of G5-$(EPTPA)_{111}$: A 20% molar excess (per terminal amine on the dendrimer) of EPTPA-bz-NCS (1.3 g, 2 mmol) was dissolved in H_2O (25 mL) and the pH adjusted to 7 with 1 M LiOH. A G5-$(NH_2)_{128}$ dendrimer solution (7.88 g, 4.77 w/w% in water, 1.67 mmol of NH_2 groups) was slowly added. The slightly cloudy solution (pH ~ 8.5) was stirred at 30 °C for 5 days and then filtered through a 0.45 μm disposable filter. The resulting clear yellow solution was evaporated to dryness and the solid was redissolved in H_2O (30 mL). Free chelate was removed by ultrafiltration using Centriprep YM10 centrifugal filter devices. The retentates were ultrafiltered twice with H_2O (20 mL). The final retentates were combined and evaporated to dryness to give the product as a white solid (1.27 g).

Synthesis of G7-$(EPTPA)_{253}$ and G9-$(EPTPA)_{1157}$: They were obtained in a similar manner as G5. A slight change in the purification after the first ultrafiltration was performed; the retentates were washed twice with 0.1 M NaCl and twice with H_2O.

Assessment of Gd^{III}-loading on the dendrimers: The number of chelate groups linked to the dendrimer surface was determined by classical complexometric titrations for the three different generations. The dendrimer solution was titrated by $GdCl_3$ (G5; buffered with urotropin, pH 6.0, xylenol orange indicator), $ZnCl_2$ (G7, NH_4^+/NH_3 buffer, pH 10.0, eriochrome black T and methyl orange as indicator) and $CaCl_2$ (G9; in NaOH solution pH 12.0, murexide indicator). The formation of the EPTPA complexes was instantaneous. The titration with Gd^{3+} could not be applied for the higher generation dendrimers, since in solutions of G7 and G9, buffered with urotropin and containing xylenol orange, a deep purple precipitate appeared immediately on addition of the first drop of Gd^{3+}. It could be the result of intercalation of the indicator into the dendrimer; however, we did not investigate the nature of the precipitation. It has to be noted that no precipitation occurs in the absence of the indicator and urotropin.

For the G5 and G7 dendrimers, the integration of the ^1H NMR spectrum (benzyl region vs. the total alkyl region) also gave an estimation of the average loading (88 and 53%, respectively). It was also in good agreement with the elemental analysis (C, H, N, S and O).

Sample preparation: The Gd^{III} (for ^{17}O NMR, NMRD and EPR) and Eu^{III} complexes (for UV/Vis) were prepared by mixing equimolar amounts of $Gd(ClO_4)_3$ or $Eu(ClO_4)_3$ and ligand in water. A slight ligand excess (5%) was used. $Gd(ClO_4)_3$, $Eu(ClO_4)_3$ and $Y(ClO_4)_3$ stock solutions were made by dissolving Ln_2O_3 in a slight excess of $HClO_4$ (Merck, p.a., 60%) in double distilled water, followed by filtration. The pH of the stock solution was adjusted to 5.5 by addition of Ln_2O_3 and its concentration was determined by titration with Na_2H_2EDTA solution using xylenol orange as indicator. For the measurements at physiological pH, 0.250 M HEPES was added to reach a final pH of 7.4 and a concentration of

0.05 M. For all other solutions (for ^{17}O NMR, NMRD, UV/Vis and EPR), the pH was adjusted by adding known amounts of $HClO_4$ or NaOH. The absence of free metal was checked in each sample by a xylenol orange test at pH around 6. The reference samples (diamagnetic Y^{III} analogues at pH 6.0 and 9.9) and the Gd^{III} complexes used for the ^{17}O NMR measurements were enriched to 1% with ^{17}O-enriched water (Isotrade GmbH) to improve sensitivity. G7 and G9 contain NaCl originating from the purification; the ionic strength was fixed to 0.1 M NaCl for each sample of the G5 dendrimer. For each sample, the concentration of the Gd^{III} ion was checked by ICP-AES.

The composition of the samples was as follows:

G5-(GdEPTPA)$_{111}$: ^{17}O NMR: 0.02625 mol kg^{-1}, pH 9.9; 0.02608 mol kg^{-1}, pH 6.0; ^{1}H NMRD: 0.00464 M, pH 7.4 (HEPES 0.050 M) (variable temperature); 0.00011 M , pH 7.4 (variable HEPES equivalent study); 0.0028–0.0031 M, pH 7.4 (HEPES 0.045 M, variable NaCl concentration study); 0.00464 M, pH 7.4 (HEPES 0.050 M, (1 Gd^{III}:1 EPTPA)), 0.00131 M, pH 7.4 (HEPES 0.050 M, (1 Gd^{III}:4 EPTPA)); 0.00311 M (variable pH study); 0.00238 M, pH 9.8 and 0.00190 M, pH 5.9. EPR: 0.00505 mol kg^{-1}, pH 6.0 (X-band); 0.02018, pH 6.0 (Q band); 0.02608 mol kg^{-1}, pH 9.8.

G5-(EuEPTPA)$_{115}$: UV/Vis: 0.013 M, pH 9.9 and 6.4.

G7-(GdEPTPA)$_{253}$: NMRD: 0.00462 M, pH 7.4 (HEPES 0.050 M); 0.00390 M (variable pH study); 0.00462 M, pH 7.4 (HEPES 0.050 M, (1 Gd^{III}:1 EPTPA)), 0.00153 M, pH 7.4 (HEPES 0.050 M, (1 Gd^{III}:4 EPTPA)).

G9-(GdEPTPA)$_{1157}$: NMRD: 0.00592 M, pH 7.4 (HEPES 0.050 M); 0.00108 M (variable pH study).

UV-visible spectroscopy: The absorbance spectra of G5-(EuEPTPA)$_{111}$ were recorded at 25 °C on a Perkin–Elmer Lambda 19 spectrometer. The measurements were done using thermostatisable cells with a 1 cm optical path length at $\lambda = 575.0$–585.0 nm.

^{17}O NMR measurements: Transverse and longitudinal ^{17}O relaxation rates and chemical shifts were measured for temperatures between 272 and 365 K. The data were recorded on Bruker DPX and ARX 400 (9.4 T, 54.2 MHz) and Bruker AC-200 spectrometers (4.7 T, 27.1 MHz). Bruker VT 3000 temperature control units were used to maintain a constant temperature, which was measured by a substitution technique. The samples were sealed in glass spheres, fitting into 10 mm NMR tubes, in order to eliminate susceptibility corrections to the chemical shifts. Longitudinal relaxation rates, $1/T_1$, were obtained by the inversion recovery method and transverse relaxation rates, $1/T_2$, were measured by the Carr–Purcell–Meiboom–Gill spin-echo technique. As external references, we used G5-(YEPTPA)$_{111}$ at concentrations and pHs identical to those of the Gd^{III} complexes.

NMRD (nuclear magnetic relaxation dispersion) spectroscopy: The $1/T_1$ NMRD profiles measurements were performed on a Stelar Spinmaster FFC fast field cycling relaxometer covering a continuum of magnetic fields from 2.35×10^{-4} to 0.47 T (corresponding to a proton Larmor frequency range 0.01–20 MHz) equipped with a VTC90 temperature control unit. The temperature was fixed by a gas flow. At higher fields, the ^{1}H relaxivity measurements were performed on Bruker Minispecs mq30 (30 MHz), mq40 (40 MHz) and mq60 (60 MHz) and on Bruker 50 MHz (1.18 T), 100 MHz (2.35 T) and 200 MHz (4.70 T) cryomagnets connected to a Bruker AC-200 console. In each case, the temperature was measured by a substitution technique.

EPR spectroscopy: The spectra were recorded in a conventional Elexsys spectrometer E500 at X-band (9.4 GHz) and Q-band (34.6 GHz). A controlled nitrogen gas flow was used to maintain a constant temperature, which was measured by a substitution technique.

Dynamic light scattering: The hydrodynamic diameter of G5-(GdEPTPA)$_{111}$ was determined by a light-scattering experiment. A solution of G5-(GdEPTPA)$_{111}$ ($c_{Gd} = 6$ mM, pH 6.7) in water was passed through a filter of 0.2 μm pore-size to remove dust from the sample. Dynamic light-scattering measurements were performed at 22.0 °C in a toluene bath at a scattering angle of 90°, using a two-photomultiplier instrument with a light source constituted by a 5 mW He-Ne laser (632.8 nm emission). The measurements were performed as previously described.[65]

Gel-permeation chromatography: High-performance liquid chromatography (HPLC) with a PSS-Novema 10 μm linear column was performed on solutions of the G5-(GdEPTPA)$_{111}$ dendrimer. Eluting peaks were detected by means of UV absorption at 230 nm. The dendrimer was eluted in aqueous 0.1 M NaCl/0.01 M NaOH and the flow rate was 1 mL min^{-1}. Experiments were performed at 23 °C.

Data analysis: The least-squares fits on the ^{17}O NMR and NMRD relaxation data were performed with the Visualiseur/Optimiseur programs on a Matlab platform version 5.3.[66,67]

Acknowledgements

We are grateful to Lothar Helm and Gaëlle Nicolle for helpful discussions. We thank Meriem Benmelouka for recording the EPR spectra, Alexander Schiller for the ICP-AES measurements and Robin Humphry-Baker for his help with dynamic light-scattering measurements. This research was financially supported by the Swiss National Science Foundation and the Office for Education and Science (OFES), it was carried out in the frame of the EC COST Action D18 and the European-funded EMIL programme (LSHC-2004-503569).

[1] U. Boas, P. M. H. Heegaard, *Chem. Soc. Rev.* **2004**, *33*, 43–63.
[2] S. E. Stiriba, H. Frey, R. Haag, *Angew. Chem.* **2002**, *114*, 1385–1390; *Angew. Chem. Int. Ed. Eng.* **2002**, *41*, 1329–1334.
[3] D. Luo, K. Haverstick, N. Belcheva, E. Han, W. M. Saltzman, *Macromolecules* **2002**, *35*, 3456–3462.
[4] T. K. Lindhorst, *Top. Curr. Chem.* **2002**, *218*, 201–235.
[5] N. Rockendorf, T. K. Lindhorst, *Top. Curr. Chem.* **2001**, *217–218*, 201–238.
[6] M. Witvrouw, V. Fikkert, W. Pluymers, B. Matthews, K. Mardel, D. Schols, J. Raff, Z. Debyser, E. De Clercq, G. Holan, C. Pannecouque, *Mol. Pharmacol.* **2000**, *58*, 1100–1108.
[7] C. Z. Chen, S. L. Cooper, *Biomaterials* **2002**, *23*, 3359–3368.
[8] C. Z. Chen, N. C. Beck-Tan, P. Dhurjati, T. K. van Dyk, R. A. LaRossa, S. L. Cooper, *Biomacromolecules* **2000**, *1*, 473–480.
[9] S. H. Battah, C. E. Chee, H. Nakanishi, S. Gerscher, A. J. MacRobert, C. Edwards, *Bioconjugate Chem.* **2001**, *12*, 980–988.
[10] H. B. Mekelburger, W. Jaworek, F. Vögtle, *Angew. Chem.* **1992**, *104*, 1609–1614; *Angew. Chem. Int. Ed. Engl.* **1992**, *31*, 1571–1576.
[11] R. Esfand, D. A. Tomalia, *Drug Discovery Today* **2001**, *6*, 427–436.
[12] D. A. Tomalia, B. Huang, D. R. Swanson, H. M. Brothers, J. W. Klimash, *Tetrahedron* **2003**, *59*, 3799–3813.
[13] J. C. Roberts, M. K. Bhalgat, R. T. Zera, *J. Biomed. Mater. Res.* **1996**, *30*, 53–65.
[14] "Relaxivity of Gadolinium(III) Complexes: Theory and Mechanism": É. Tóth, A. E. Merbach in *The Chemistry of Contrast Agents in Medical Magnetic Resonance Imaging*, (Eds.: É. Tóth, A. E. Merbach) Wiley, Chichester, **2001**.
[15] M. W. Brechbiel, R. A. Star, H. Kobayashi, U. S. Pat. Appl. Publ. **2004**, 2004037777.
[16] H. Kobayashi, N. Sato, S. Kawamoto, T. Saga, A. Hiraga, T. Ishimori, J. Konishi, K. Togashi, M. W. Brechbiel, *Magn. Reson. Med.* **2001**, *46*, 579–585.
[17] L. J. M. Kroft, A. de Roos, *J. Magn. Reson. Imaging* **1999**, *10*, 395–403.
[18] R. C. Brasch, *Magn. Reson. Med.* **1991**, *22*, 282–287.
[19] R. C. Brasch, C. Pham, D. M. Shames, T. P. Roberts, K. van Dijke, N. van Bruggen, J. S. Mann, S. Ostrowitzki, O. Melnyk, *J. Magn. Reson. Imaging* **1997**, *7*, 68–74.
[20] C. F. van Dijke, R. C. Brasch, T. P. Roberts, N. Weidner, A. Mathur, D. M. Shames, J. S. Mann, F. Demsar, P. Lang, H. C. Schwickert, *Radiology* **1996**, *198*, 813–818.
[21] É. Tóth, L. Helm, K. E. Kellar, A. E. Merbach, *Chem. Eur. J.* **1999**, *5*, 1202–1211.

[22] É. Tóth, I. van Uffelen, L. Helm, A. E. Merbach, D. Ladd, K. Briley-Saebo, K. E. Keller, *Magn. Reson. Chem.* **1998**, *36*, S125–S134.
[23] F. A. Dunand, É. Tóth, R. Hollister, A. E. Merbach, *J. Biol. Inorg. Chem.* **2001**, *6*, 247–255.
[24] G. P. Yan, R. X. Zhuo, M. Y. Xu, X. Zhang, L. Y. Li, M. L. Liu, C. H. Ye, *Polym. Int.* **2002**, *51*, 892–898.
[25] M. G. Duarte, M. H. Gil, J. A. Peters, J. M. Colet, L. Vander Elst, R. N. Muller, C. F. G. C. Geraldes, *Bioconjugate Chem.* **2001**, *12*, 170–177.
[26] E. C. Wiener, M. W. Brechbiel, H. Brothers, R. L. Magin, O. A. Gansow, D. A. Tomalia, P. C. Lauterbur, *Magn. Reson. Med.* **1994**, *31*, 1–8.
[27] É. Tóth, D. Pubanz, S. Vauthey, L. Helm, A. E. Merbach, *Chem. Eur. J.* **1996**, *2*, 1607–1615.
[28] L. D. Margerum, B. K. Campion, M. Koo, N. Shargill, J.-J. Lai, A. Marumoto, P. C. Sontum, *J. Alloys Compd.* **1997**, *249*, 185–190.
[29] L. H. Bryant. Jr., M. W. Brechbiel, C. Wu, J. W. M. Bulte, V. Herynek, J. A. Frank, *J. Magn. Reson. Imaging* **1999**, *9*, 348–352.
[30] G. M. Nicolle, É. Tóth, H. Schmitt-Willich, B. Radüchel, A. E. Merbach, *Chem. Eur. J.* **2002**, *8*, 1040–1048.
[31] J. P. André, É. Tóth, H. Fischer, A. Seelig, H. R, Mäcke, A. E. Merbach, *Chem. Eur. J.* **1999**, *5*, 2977–2983.
[32] G. M. Nicolle, É. Tóth, K. P. Eisenwiener, H. R. Mäcke, A. E. Merbach, *J. Biol. Inorg. Chem.* **2002**, *7*, 757–769.
[33] R. Hovland, C. Gløgård, A. J. Aasen, J. Klaveness, *Org. Biomol. Chem.* **2003**, *1*, 644–647.
[34] K. Kimpe, T. N. Parac-Vogt, S. Laurent, C. Piérart, L. Vander Elst, R. N. Muller, K. Binnemans, *Eur. J. Inorg. Chem.* **2003**, *16*, 3021–3027.
[35] A. Accardo, D. Tesauro, P. Roscigno, E. Gianolio, L. Pduano, G. D'Errico, C. Pedone, G. Morelli, *J. Am. Chem. Soc.* **2004**, *126*, 3097–3107.
[36] "Protein-Bound Metal Chelates": S. Aime, M. Fasano, E. Terreno, M. Botta in *The Chemistry of Contrast Agents in Medical Magnetic Resonance Imaging* (Eds.: É. Tóth, A. E. Merbach) Wiley, Chichester, **2001**, p. 193.
[37] S. Aime, M. Botta, M. Fasano, G. S. Crich, E. Terreno, *J. Biol. Inorg. Chem.* **1996**, *1*, 312–319.
[38] R. B. Lauffer, D. J. Parmalee, S. U. Dunham, H. S. Ouellet, R. P. Dolan, S. Witte, T. J. McMurry, R. C. Walowitch, *Radiology* **1998**, 207, 529–538.
[39] P. Caravan, N. J. Cloutier, M. T. Greenfield, S. A. McDermid, S. U. Dunham, J. W. M. Bulte, J. C. Amedio, Jr., R. J. Looby, R. M. Supkowski, W. DeW Horrocks, Jr., T. J. McMurry, R. B. Lauffer, *J. Am. Chem. Soc.* **2002**, *124*, 3152–3162.
[40] R. Ruloff, É. Tóth, R. Scopelliti, R. Tripier, H. Handel, A. E. Merbach, *Chem. Commun.* **2002**, *22*, 2630–2631.
[41] S. Laus, R. Ruloff, É. Tóth, A. E. Merbach, *Chem. Eur. J.* **2003**, *9*, 3555–3566.
[42] E. T. Clarke and A. E. Martell, *Inorg. Chim. Acta* **1991**, *190*, 27–36.
[43] E. T. Clarke and A. E. Martell, *Inorg. Chim. Acta* **1991**, *190*, 37–46.
[44] D. T. Corson, C. F. Meares, *Bioconjugate Chem.* **2000**, *11*, 292–299.
[45] L. Burai, É. Tóth, A. Sour, A. E. Merbach, *Inorg. Chem.*, in press.
[46] G. M. Nicolle, F. Yerly, D. Imbert, U. Böttger, J.-C, Bünzli, A. E. Merbach, *Chem. Eur. J.* **2003**, *9*, 5453–5467.
[47] É. Tóth, L. Helm, A. E. Merbach, R. Hedinger, K. Hegetschweiler, A. Jánossy, *Inorg. Chem.* **1998**, *37*, 4104–4113.
[48] G. M. Nicolle, L. Helm, A. E. Merbach, *Magn. Reson. Chem.* **2003**, *41*, 794–799.
[49] N. Graeppi, D. H. Powell, G. Laurenczy, L. Zékány, A. E. Merbach, *Inorg. Chim. Acta* **1995**, *235*, 311–326.
[50] G. Lipari, S. Szabo, *J. Am. Chem. Soc.* **1982**, *104*, 4546–4559.
[51] G. Lipari, S. Szabo, *J. Am. Chem. Soc.* **1982**, *104*, 4559–4570.
[52] I. Bertini, O. Galas, C. Luchinat, G. Parigi, *J. Magn. Reson. Ser. A* **1995**, *113*, 151–158.
[53] S. Rast, P. H. Fries, E. Belozirsky, *J. Chem. Phys.* **2000**, *113*, 8724–8735.
[54] S. Rast, A. Borel, L. Helm, E. Belozirsky P. H. Fries, A. E. Merbach, *J. Am. Chem. Soc.* **2001**, *123*, 2637–2644.
[55] D. H. Powell, O. M. Ni Dhubhghaill, D. Pubanz, L. Helm, Y. S. Lebedev, W. Schlaepfer, A. E. Merbach, *J. Am. Chem. Soc.* **1996**, *118*, 9333–9346.
[56] F. Dunand, A. Borel, A. E. Merbach, *J. Am. Chem. Soc.* **2002**, *124*, 710–7016.
[57] F. Yerly, K. I. Hardcastle, L. Helm, S. Aime, M. Botta, A. E. Merbach, *Chem. Eur. J.* **2002**, *8*, 1031–1039.
[58] Z. Jászberényi, personal communication.
[59] P. Welch, M. Muthukumar, *Macromolecules* **1998**, *31*, 5892–5897.
[60] T. Terao, T. Nakayama, *Macromolecules* **2004**, *37*, 4686–4694.
[61] I. Lee, B. D. Athey, A. W. Wetzel, W. Meixner, J. R. Baker Jr., *Macromolecules* **2002**, *35*, 4510–4520.
[62] M. S. Diallo, S. Christie, P. Swaminathan, L. Balogh, X. Shi, W. Um, C. Papelis, W. A. Goddard III, J. H. Johnson Jr., *Langmuir* **2004**, *20*, 2640–2651.
[63] R. Ruloff, G. van Koten, A. E. Merbach, *Chem. Commun.* **2004**, 842–843.
[64] J. B. Livramento, É. Tóth, A. Sour, A. Borel, A. E. Merbach, R. Ruloff, *Angew. Chem.* **2005**, *117*, 1504–1508; *Angew. Chem. Int. Ed.* **2005**, *44*, 1480–1484.
[65] R. Humphry-Baker, D. H. Thompson, Y. Lei, M. J. Hope, J. K. Hurst, *Langmuir* **1991**, *7*, 2592–2601.
[66] F. Yerly, VISUALISEUR 2.3.4, Lausanne (Switzerland), **1999**.
[67] F. Yerly, OPTIMISEUR 2.3.4, Lausanne (Switzerland), **1999**.

Received: December 23, 2004
Published online: March 17, 2005